J Mater Sci (2009) 44:4003–4012
DOI 10.1007/s10853-009-3551-3

Evaluation and visualization of the percolating networks in multi-wall carbon nanotube/epoxy composites

Li Chang · Klaus Friedrich · Lin Ye · Patricio Toro

Received: 2 February 2009 / Accepted: 5 May 2009 / Published online: 22 May 2009

Abstract In this study, epoxy-based nanocomposites containing multi-wall carbon nanotubes (CNTs) were produced by a calendering approach. The electrical conductivities of these composites were investigated as a function of CNT content. The conductivity was found to obey a percolation-like power law with a percolation threshold below 0.05 vol.%. The electrical conductivity of the neat epoxy resin could be enhanced by nine orders of magnitude, with the addition of only 0.6 vol.% CNTs, suggesting the formation of a well-conducting network by the CNTs throughout the insulating polymer matrix. To characterize the dispersion and the morphology of CNTs in epoxy matrix, different microscopic techniques were applied to characterize the dispersion and the morphology of CNTs in epoxy matrix, such as atomic force microscopy, transmission electron microscopy, and scanning electron microscopy (SEM). In particular, the charge contrast imaging in SEM allows a visualization of the overall distribution of CNTs at a micro-scale, as well as the identification of CNT bundles at a nano-scale. On the basis of microscopic investigation, the electrical conduction mechanism of CNT/epoxy composites is discussed.

L. Chang (✉) · L. Ye
Centre for Advanced Materials Technology, School of Aerospace, Mechanical and Mechatronic Engineering, The University of Sydney, Sydney, NSW 2006, Australia
e-mail: l.chang@usyd.edu.au

K. Friedrich
Institute for Composite Materials, University of Kaiserslautern, Kaiserslautern 67663, Germany

K. Friedrich
King Saud University, Riyadh, Saudi Arabia

P. Toro
Facultad de Ciencias Físicasy Matemáticas, Casilla 2777, Universidad de Chile, Santiago, Chile

Introduction

Since their discovery in the 1990s, carbon nanotubes (CNTs), including single wall CNTs and multi-wall CNTs, have attracted increasing attention throughout the academic and industrial world [1, 2]. CNTs exhibit excellent mechanical performance, high electrical and thermal conductivity as well as chemical stability, thus making them ideal fillers in multifunctional polymer nanocomposites [3, 4]. One of the promising applications of CNTs is to achieve electron conduction in polymers using very low filler contents without sacrificing other inherent properties of the polymer matrix [5]. Such conductive polymer nanocomposites can be used for, e.g., electrostatic discharge and electromagnetic interference shielding [6].

To describe the electrical percolation behavior of insulating polymers filled with conducting fillers, a percolation theory is frequently applied. The lowest filler concentration needed for the insulator–conductor transition in composites is defined as the percolation threshold. The conductivity for the composites with filler contents in the vicinity of the percolation threshold is governed by the following scaling law [7, 8]:

$$\sigma_c = \sigma_f \cdot (p - p_c)^t, \quad (1)$$

where σ_c is the electrical conductivity of the composite, σ_f the conductivity of the filler, p the volume fraction of filler, p_c the percolation threshold, and t is the critical exponent for the conductivity. Many studies have proved both experimentally and theoretically that the percolation

threshold is dependent on the morphology of the conductive fillers, such as shape, size, and aspect (length-to-diameter) ratio [9–12]. In particular, the value of the percolation threshold can be significantly reduced by increasing the aspect ratio of fillers [11–14]. The critical exponent t, however, is determined by the dimensionality of the sample with universal values ~ 1.3 and ~ 2 in two and three dimensions, respectively [9, 15]. Although the statistical percolation approach has been successfully applied in diverse applications, it was noted that the percolation theory is inadequate for interpreting the electrical conductive behavior of polymers filled with CNTs [16, 17]. The experimental percolation thresholds for CNT-filled nanocomposites can be orders of magnitude lower than the theoretical values [18–20]. The ultra low electrical percolation threshold is normally attributed to a "network-like-structure" of CNTs [21–24]. Such a CNT network was also expected to enhance the nanocomposite's mechanical properties and other multifunctional performances, e.g., thermal conductivity [25, 26]. However, up to now, the detailed knowledge of the CNT structure in a polymeric matrix is still very limited, due to the fact that it is difficult to directly observe CNT dispersion by using traditional microscopy techniques, which significantly hinders a deep understanding of the structure–property relationships of CNT-filled polymer composites.

This study was aimed to investigate both the electrical conductivity behavior of CNT/epoxy composites and the effect of the formation of CNTs network. Multi-wall CNTs were dispersed in an epoxy matrix by using a calendering approach. The electrical property of CNT/epoxy composites was examined as a function of CNT content and analyzed with respect to aspects of the percolation theory. To characterize the dispersion state of CNTs, different microscopic techniques such as atomic force microscopy (AFM), transmission electron microscopy (TEM), and scanning electron microscopy (SEM) were applied. In particular, charge contrast imaging in SEM was utilized to visualize the CNT structure in epoxy nanocomposites.

Materials and experimental details

Materials preparation

The multi-wall CNTs were provided by BAYER (Baytubes C150P), with an outer diameter of ~ 15 nm, an inner diameter of ~ 4 nm, and a length of a few microns. Figure 1 shows the scanning electron micrographs of the as-received CNTs, which are highly agglomerated in the form of powder particles.

To break up the agglomerates, the CNT powders were mixed into the epoxy resin (Araldite LY 564) at room temperature using a vacuum dissolver (Dispermat, VMA-Getzmann GmbH) in the beginning. Further dispersion was carried out with the help of a three-roll calender (TD1-3M, Toshin Co., Ltd., Japan). The schematic of the calender configuration is shown in Fig. 2. A small gap between the rolls and a mismatch in rolling speed can result in enormous shear forces, which can effectively break up CNT agglomerates with limited breakage of the nanotubes. In the experiments, the mismatch between the angular velocity of adjacent rolls was fixed as $\omega_1:\omega_2:\omega_3 = 1:3:9$. The gap distance between the rolls was adjusted by an electronic control system and ranged from 5 to 300 μm. The mixture of CNT/resin was then collected and the hardener (Aradur HY 2954) was added and mixed using a dissolver (VMA-Getzmann GmbH, Reichshof) at 60 °C. Finally curing took place over 8 h at 140 °C in a vacuum oven.

Measurement of electrical conductivity

The electrical conductivity of epoxy nanocomposites with various CNT contents (0.01, 0.05, 0.1, 0.2, 0.3, and 0.6 vol.%) was measured at room temperature, using a

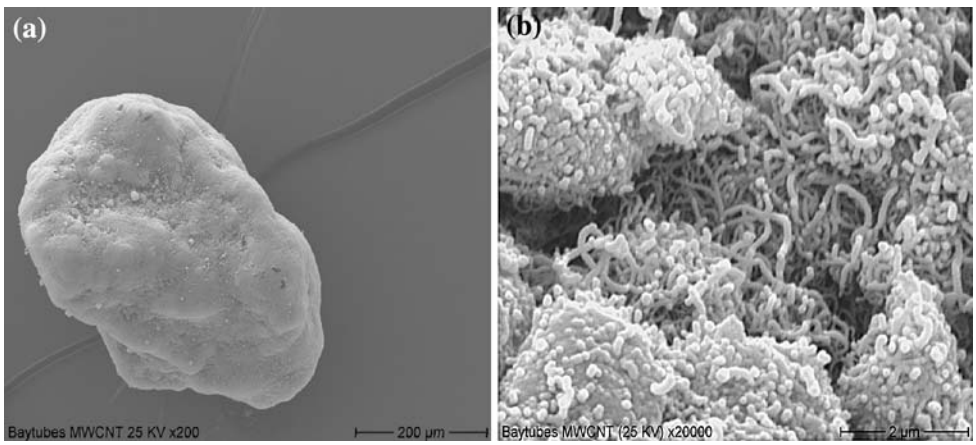

Fig. 1 SEM micrographs of the as-received nanotubes: **a** entanglement of CNTs at micro-, and **b** nano-scales

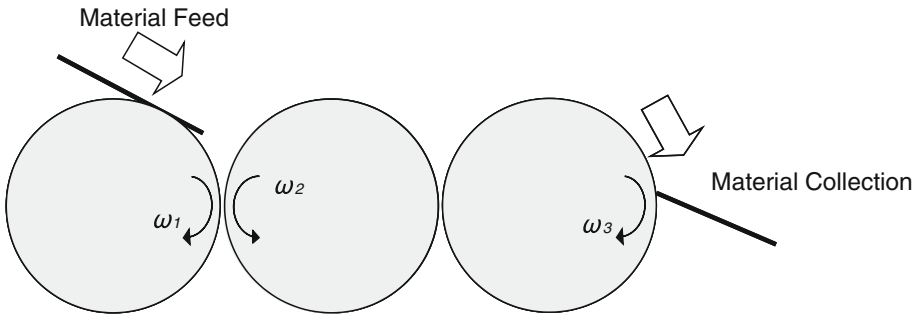

Fig. 2 Schematic diagram of the configuration of a three-roll calender used for dispersion of CNTs in epoxy resin

surface resistivity testing device (Hiresta UP, Mitsubishi Chemicals), according to ASTM D-257. The electrometer covers a range of surface resistance between 10^4 and 10^{14} Ohms. In this study, the surface resistivity was measured using a ring electrode (UR-SS Type, Mitsubishi Chemicals) by applying a constant voltage across the surface of the sample. Then, the electrical conductivity could be determined by the following equation:

$$\sigma = \frac{IL}{UA}, \tag{2}$$

where I is the resultant current, U the voltage potential, A the surface of the electrode, and L the distance between the electrodes.

Electron microscopy

To examine the CNT network in epoxy composites, different microscopic techniques were applied. TEM imaging was performed with a Zeiss 902. The samples were cut to thin slices (90 nm) using an ultramicrotome with a diamond knife. The slices were then collected on grids and observed with the TEM. The topography of CNT/epoxy composites was examined by the use of an AFM (Digital Instruments). CNTs were identified with both height and phase contrast pictures. The high-resolution SEM images were taken with a ZEISS Supra^{TM} 40VP. The fracture surfaces of CNT/epoxy composites were examined without an additional coating to avoid any mask over the nanotubes and to allow a contrast imaging between the conductive CNTs and the dielectric epoxy matrix. A low acceleration voltage of 0.5 kV was utilized in order to reduce electron penetration and to view dispersion of CNTs on and only slightly below the specimen surface [27–29].

Results and discussion

Electrical percolation behavior of CNT/epoxy composites

The electrical conductivity results are plotted in Fig. 3 as a function of CNT concentration. An abrupt increase in the

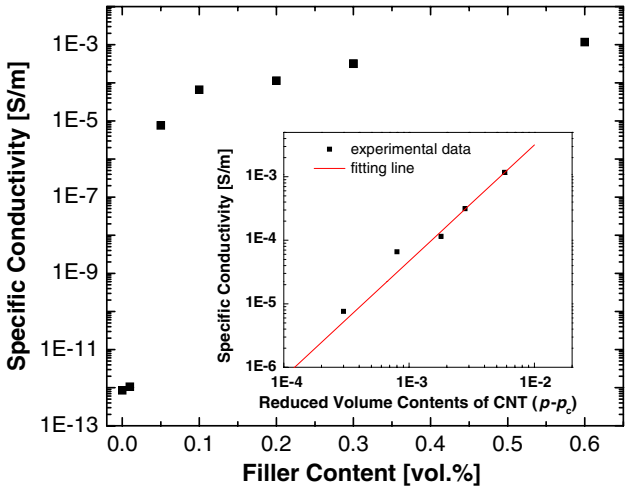

Fig. 3 Electrical conductivity of the epoxy-based nanocomposites as a function of the volume contents of CNT. *Inset*: a log–log plot of the electrical conductivity of epoxy nanocomposites as a function of $(p - p_c)$ with the fit line determined by Eq. 1

electrical conductivity was observed for CNT loadings in the range of 0.01 to 0.05 vol.%, indicating the formation of a percolating path through the CNT/epoxy system. The inset shows a linear regression fit to the specific conductivity σ_c, as a function of $(p - p_c)$ by the log–log plot. According to Eq. 1, the fit also results in a value for the saturation conductivity σ_f of 14.5 S/m and a value of 1.83 for the scaling exponent t, with a percolation threshold p_c of 0.02 vol.%.

According to the excluded volume theory, the percolation threshold for a material containing the high-aspect-ratio fillers can be calculated by the following equation [12]:

$$1 - \exp\left(-\frac{1.4V}{V_e}\right) \leq p_c \leq 1 - \exp\left(-\frac{2.8V}{V_e}\right), \tag{3}$$

where V is the volume of the individual filler, and V_e the excluded volume that is defined as the volume around an object, into which another similarly shaped object is not allowed to penetrate [11]. For the randomly oriented fiber-like fillers, V_e is determined by [11]:

$$V_e = \frac{4\pi}{3}D^3 + 2\pi D^2 L + \frac{\pi}{2}DL^2, \tag{4}$$

where D is the diameter of the fiber and L the length. The underlying idea of the excluded volume theory is that the percolation threshold is not dependent on the true volume of the object itself but its excluded volume. In the present case, when the nanotubes are simplified as straight fibers with the average dimensions of $D = 15$ nm and $L = 3$ μm, the theoretical value of p_c will be between 0.34 and 0.68 vol.%. These results are more than one order of magnitude higher than the fitting value (0.02 vol.%). Besides, it is noticed that the saturation conductivity σ_f is significantly lower than the electrical conductivity of individual multi-wall CNTs ($\sim 10^5$ S/m; [26]). Therefore, although the experimental conductivity apparently obeys the percolation-like power law, the conductive behavior of the CNT/epoxy composites cannot be fully explained by the geometrical percolation theory. It is known that the dispersion state of the tubes, as well as the nature of the interaction between tubes and polymer matrix is crucial for the conductive properties of CNT-modified polymers. In the following sections, the conductivity mechanism of CNT-reinforced epoxy composites will be further explored, especially on the basis of the morphological investigation of the CNT dispersion.

Observation of CNT networks in polymer nanocomposites

To examine the CNT dispersion in the epoxy matrix, various microscopic techniques have been applied. Figure 4 compares the TEM micrographs of CNT-filled epoxy composites, containing different CNT contents. With a high magnification, individual CNTs can be clearly viewed in the different regions (cf. Fig. 5). It is obvious that tubes are irregularly curved, and some of them are significantly agglomerated in the submicron-scale. Although TEM can clearly visualize the individual nanotubes, it is difficult to draw a conclusion concerning the global dispersion of CNTs in the nanocomposites, due to the scale limitation. In fact, as shown in Fig. 4, the CNT structure looks almost identical even with very different CNT contents.

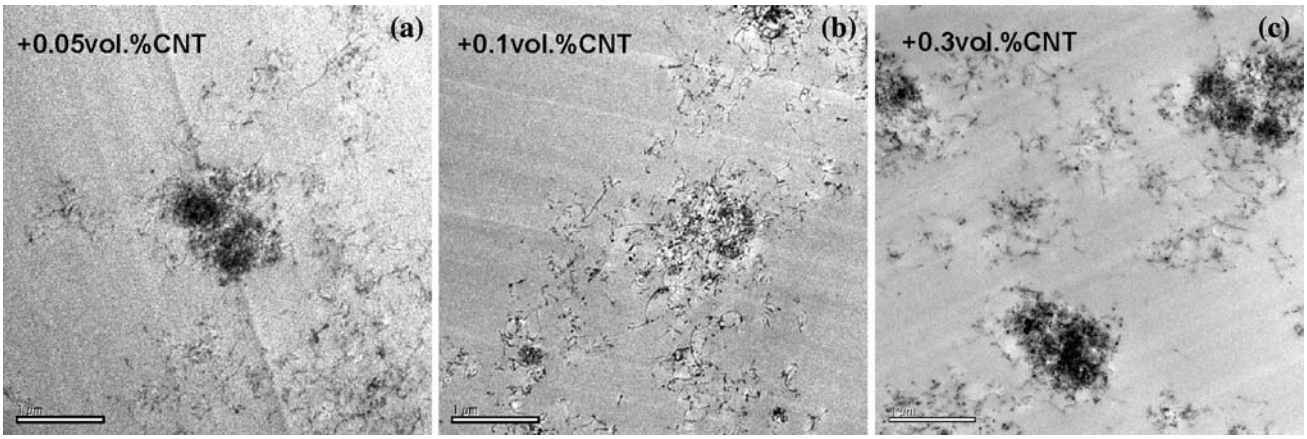

Fig. 4 TEM micrographs of epoxy-based nanocomposites with different CNT volume contents: **a** 0.05 vol.%, **b** 0.1 vol.%, **c** 0.3 vol.%

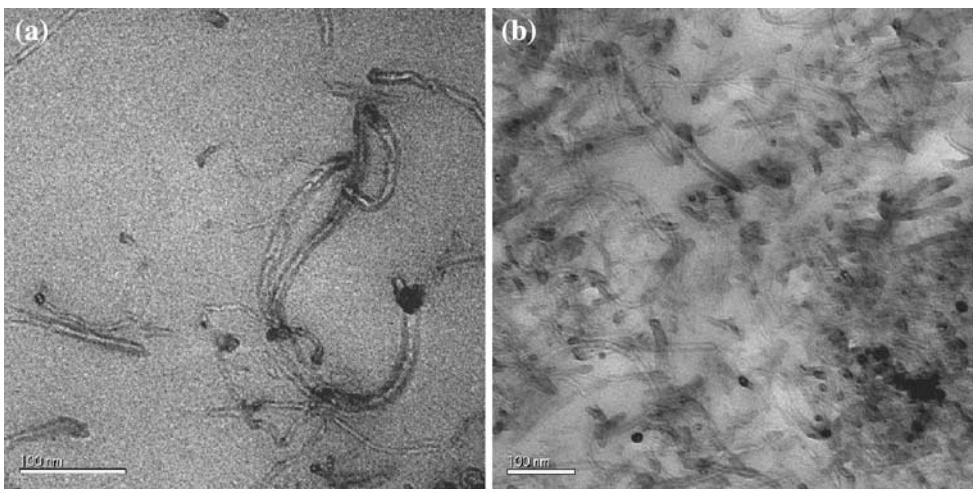

Fig. 5 TEM-images of **a** curved and **b** entangled nanotubes in a 0.3 vol.% CNT-filled epoxy composite

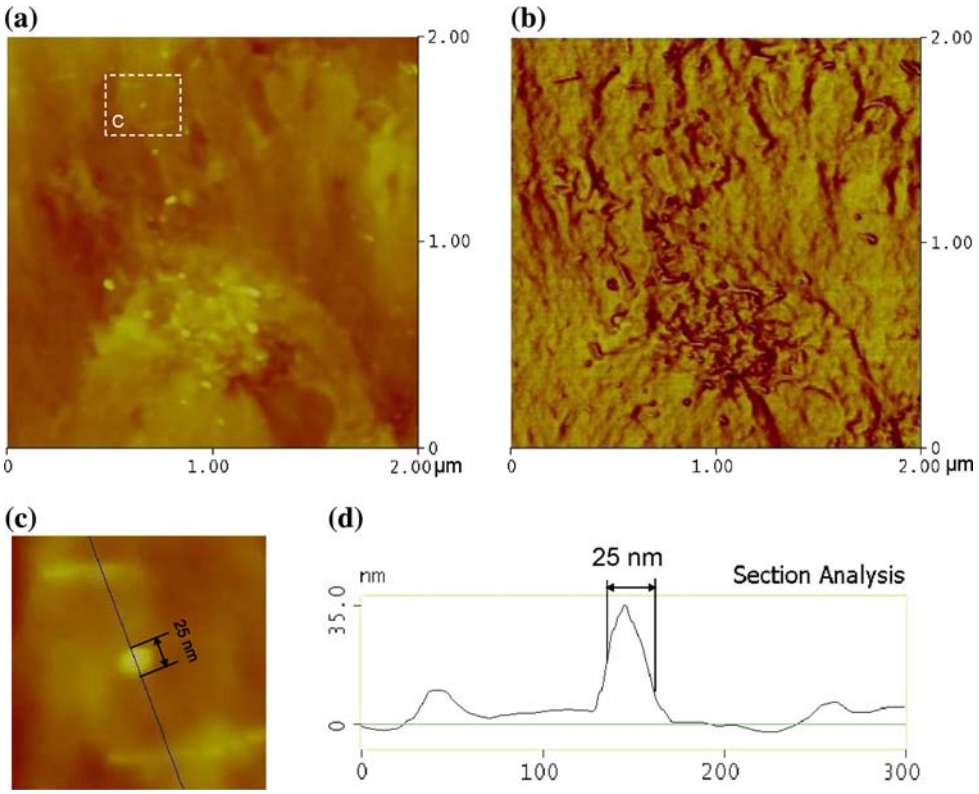

Fig. 6 AFM-images of a 0.6 vol.% CNT-filled epoxy composite: **a** height contrast, **b** phase contrast, **c** a high magnification view, and **d** a corresponding cross-sectional measurement

Figure 6 shows the AFM images of the fracture surface of epoxy nanocomposites filled with 0.6 vol.% CNT. In comparison to the TEM images, the height contrast image (Fig. 6a) shows bright dots and short lines, which may represent nanotubes pulled out of the fracture surface. The agglomeration of CNTs can be clearly seen in the phase contrast image (Fig. 6b). With a high magnification view (Fig. 6c), the width of the lines/dots can be measured, which is in reasonable agreement with the outer diameter of the CNTs (cf Fig. 6d). However, it is also difficult to view the dispersion of CNTs by AFM on a larger scale, since the scanning time will be very long in order to identify individual CNT with a high resolution. In this case, the time-dependent errors such as drift-distortion will greatly limit the quality of the AFM images.

Figure 7 illustrates a series of charge contrast SEM images of 0.3 vol.% CNT/epoxy composite with different magnifications. The CNT-rich domains appear as bright zones due to the different capabilities for charge transport which is much higher for the conductive CNTs in comparison to the dielectric polymer matrix. With higher magnification, individual CNTs and CNT-bundles can be clearly identified (cf. Fig. 7c, d). These high-resolution SEM images of CNTs are fairly comparable to those observed with TEM, e.g., Figs. 4a and 5b, which well supports the reliability of the charge contrast SEM technique. Figure 8 further compares the CNTs distribution in the composites as a function of different CNT contents. Together with Fig. 7, it was found that the CNT-rich domains were uniformly dispersed in the epoxy matrix, and the density of these domains increased with an increase in CNT content. Within these domains, however, CNTs were considerably agglomerated (cf. Figs. 4 and 7). Such CNT structure is mostly determined by the manufacturing process. In this study, the gap between calender rollers was on a micro-scale. As a result, the CNTs remained agglomerated in a submicron-scale, i.e., they formed small CNT-rich domains. In general, it is possible to improve the dispersion of CNTs in a finer scale by reducing the gap between the calender rollers, so as to increase the shear stresses for an entanglement of the nanotubes. However, a higher shear stress can also damage the nanotubes and substantially reduce their aspect ratio, which might cause a detrimental reduction in the mechanical and/or functional performances of the CNT-filled polymer composites. Hence, the manufacturing parameters have to be optimized according to the industrial demands for applications of this kind of materials.

It is obvious that the charge contrast SEM imaging is an effective technique to visualize the distribution of CNTs in polymer composites even on several length scales. This will provide a solid base to better understand the processing–structure–property relationship in CNT-filled nanocomposites. However, it should be also stated that the charging process is very complicated and that the underlying mechanism has not been fully understood. Charge

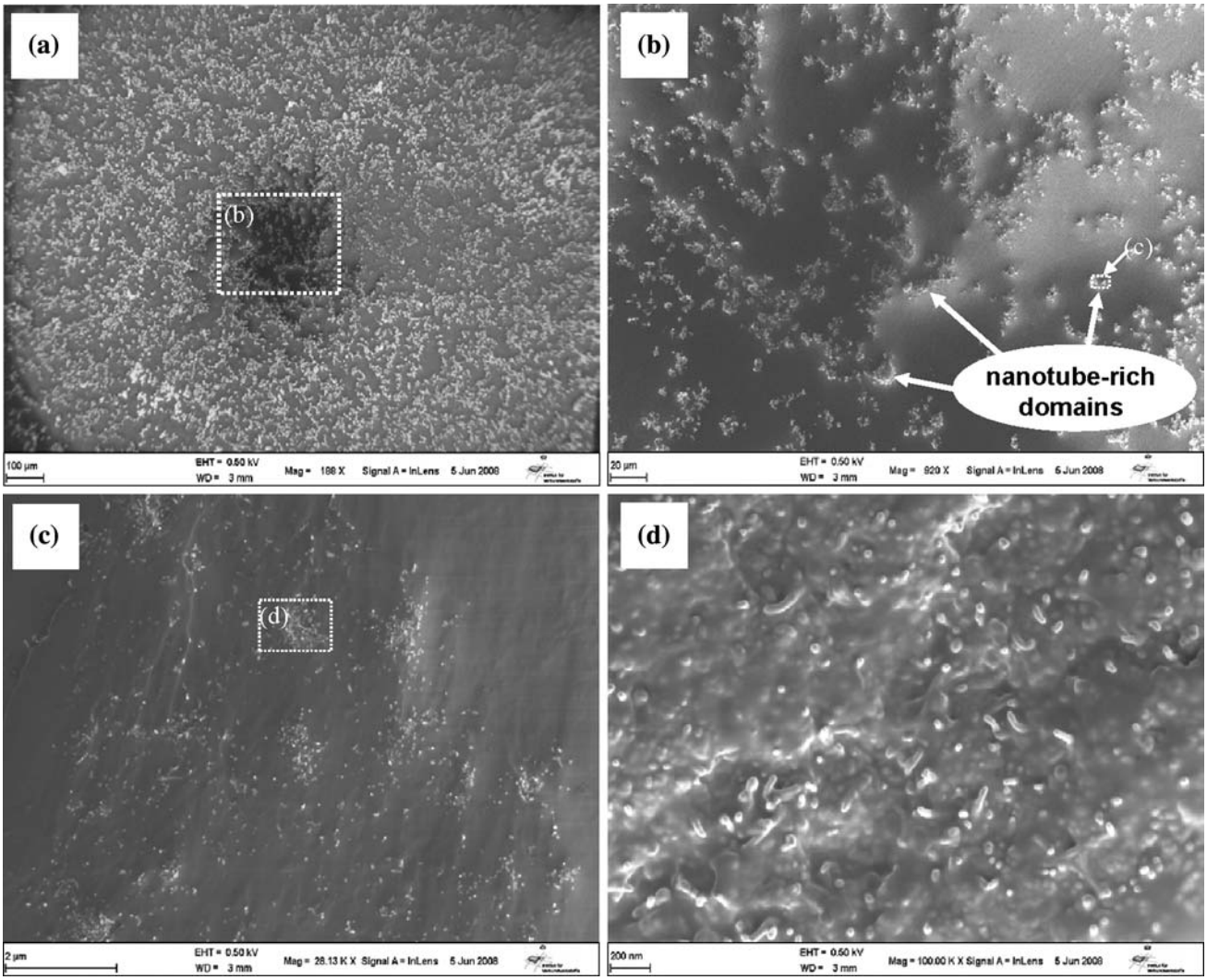

Fig. 7 Series of high-resolution SEM images of a 0.3 vol.% CNT-filled epoxy composite: **a**–**c** the dispersion of CNT at micro- and submicron-scale, **d** the agglomerated nanotubes at a nanoscale. CNTs become visible at different length scales by contrast imaging, due to the different electrical conductivities between fillers and matrix

contrast images are not only dependent on the SEM operating parameters such as acceleration voltage, working distance, and chamber pressure, but also on internal properties of the specimens [28, 29]. In the experiments, it was noticed that when the CNT content is lower than the percolation threshold, it was very difficult to obtain a stable image (cf. Fig. 8). One possible reason is the charge effect at the surface of the poorly conductive specimen. This effect is time dependent and involves dynamic processes such as electron collision, diffusion, trapping, and interactions among them. As a result, it is difficult to reach an equilibrium state. Nevertheless, up to now, the detailed model of the charging process is not available, and therefore a quantitative analysis is still very difficult. More fundamental study needs to be done to understand the charge-trapping behavior of materials with different conductive properties, which then might also significantly extend SEM applications in this field.

Discussion on the conduction mechanism

On the basis of the microscopic observations, a schematic of the CNT-distribution in an epoxy resin is illustrated in Fig. 9. It is proposed that CNTs agglomerate in nano- and submicro-scales and form discrete CNT-rich domains. However, these domains are well dispersed in the polymer matrix. When the CNT content is higher than a critical value, these domains will connect to a three-dimensional network throughout the matrix system. As a result, the macro electrical conductive behavior of CNT/epoxy nanocomposites can be well described by the statistical percolation theories. On

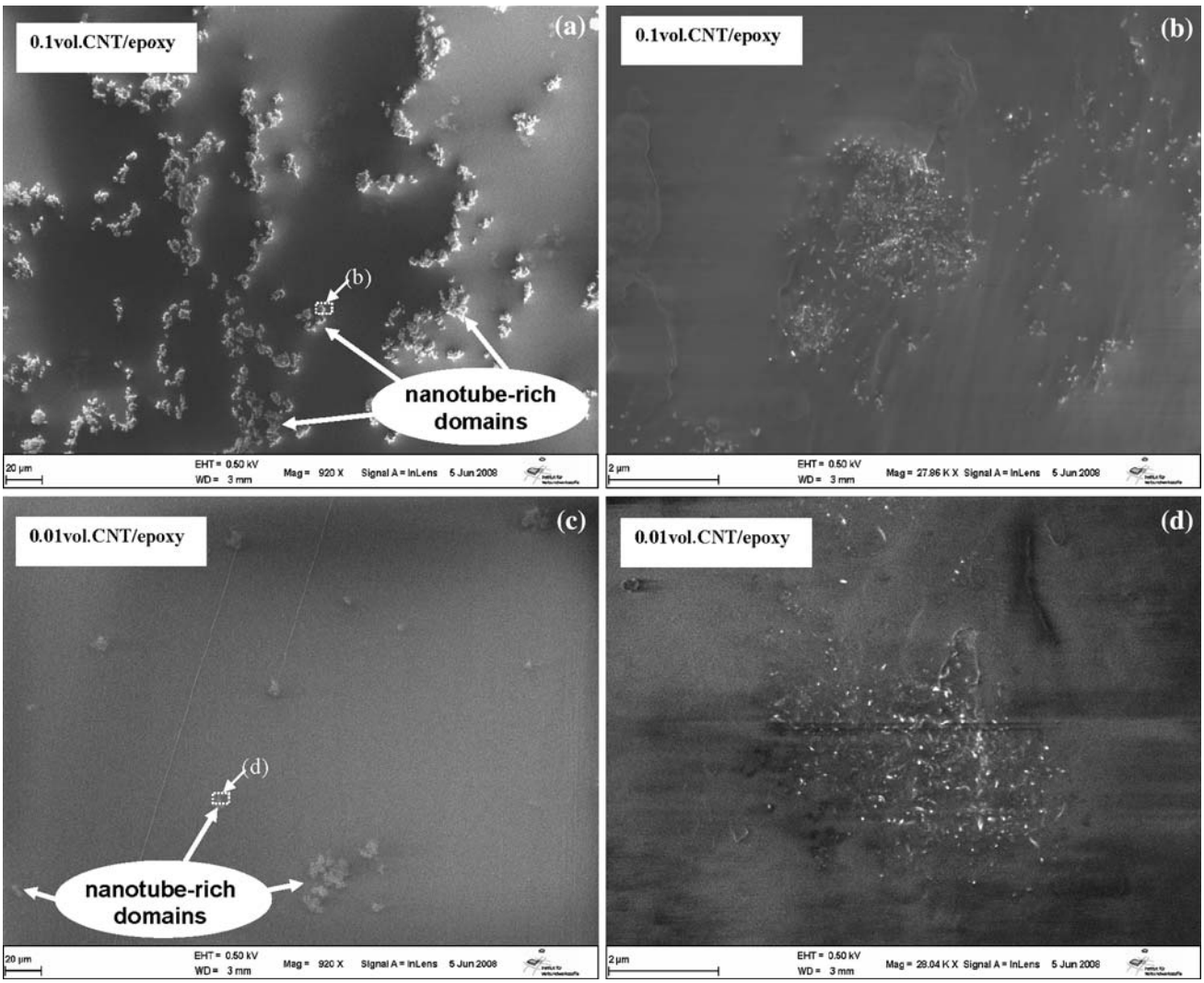

Fig. 8 Comparison of the dispersion of CNT in epoxy nanocomposites with different volume contents: **a** overview, **b** a high-magnification image of composite with 0.1 vol.% CNT, **c** overview and **d** a high-magnification image of composite with 0.01 vol.% CNT

the other hand, the local nanotube clusters may have an influence on the value of power law parameters, e.g., the scaling exponent t, due to a reduction of the effective volume fraction of dispersed CNTs. As the amount of CNT aggregation generally increases with the CNT loading, the value of the experimental t (which is 1.83) is slightly smaller than the universal value of 2. However, the model cannot fully explain that the experimental percolation threshold is greatly lower than the theoretical value predicted by the excluded volume theory. In fact, as nanotubes in polymer composites appear curved and entangled (cf. Fig. 5), this will even lead to an underestimation of the percolation threshold by the excluded volume approach because the effective length of curved tubes is shorter than that for a straight fiber [30]. Therefore, other factors must contribute to such a low percolation threshold.

It is noticed that some individual tubes are not directly touching each other but are isolated by the polymer matrix (cf. Figs. 3 and 4). This is not surprising since the CNTs were fully immersed in the epoxy resin during manufacturing process. Hence, efficient carrier transport between CNTs is blocked by polymer layers and fluctuation-induced tunneling has to be taken into account for the electrical conductive behavior of CNT-filled composites. The tunneling mechanism has been proposed to explain the percolation behavior in carbon black-polyvinylchloride system [31, 32], and it was recently introduced also to CNTs/polymer systems [33–36]. It was indicated that when nanotubes reach the electrical percolation threshold in a polymeric matrix, they need not always physically touch each other, as long as they are just close enough to allow the hopping/tunneling processes. The insulating gap between nanotubes can well explain that the experimental

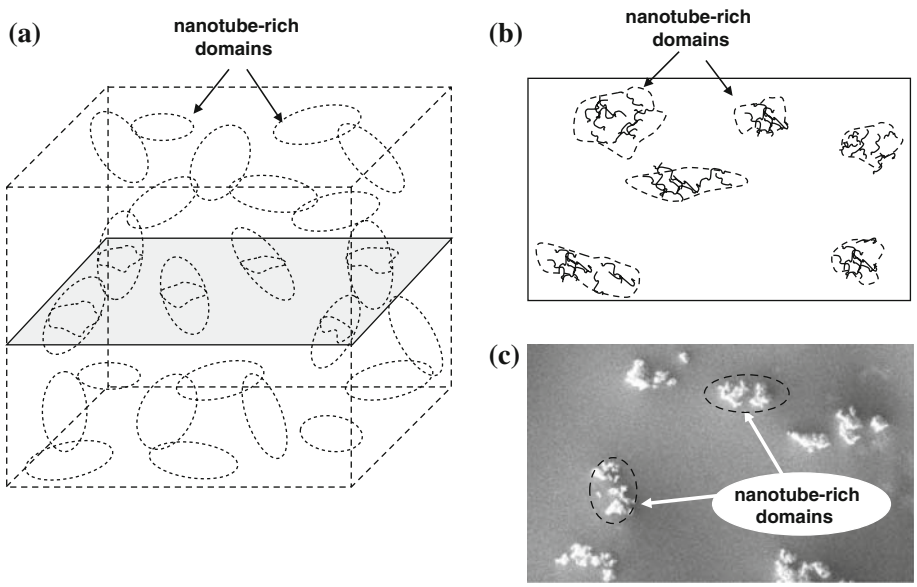

Fig. 9 **a** Schematic illustration of the three-dimensional CNT network in epoxy matrix, **b** a cross-sectional surface, comparing with **c** a charge contrast image observed by SEM

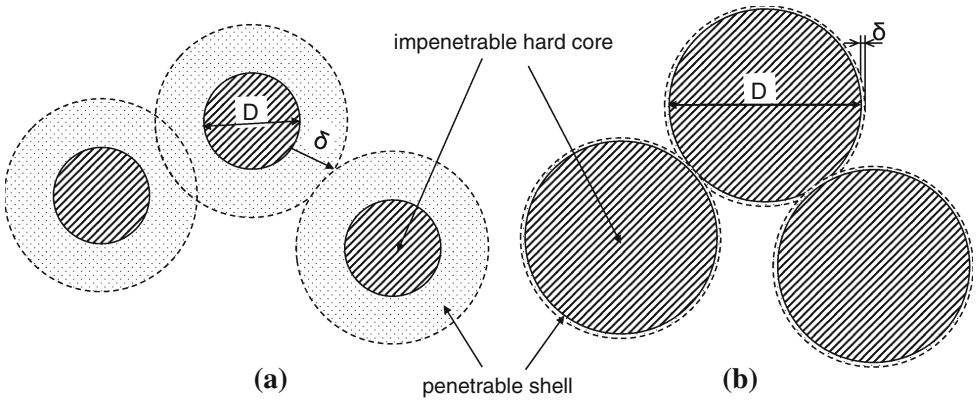

Fig. 10 Schematic illustration of the conductive fillers with different diameters covered with polymer layers: **a** $\frac{\delta}{D} = 0.5$ and **b** $\frac{\delta}{D} = 0.02$. The impenetrable hard core represents the conductive filler with a diameter of D. The penetrable layer refers to the polymer matrix with a thickness δ, equal to the possible electron hopping distance

saturation conductivity of CNT nanocomposites is always orders of magnitude lower than the electrical conductivity of individual CNTs [20, 22]. On the basis of both the tunneling theory and the geometrical percolation theory, a "hard-core" model was developed in order to represent the conductive behavior of short-fiber-filled polymer composite [13].

The schematic illustration of the "hard-core" mode is shown in Fig. 10. The conductive fillers with a diameter D are treated as impenetrable hard cores. They are covered with a permeable shell (with the thickness δ), which refers to an extended range in the polymer matrix that allows hopping of electrons. In this case, the excluded volume is dependent on $(\delta + D)$, i.e. $(1 + \delta/D)D$, rather than D. When $\delta/D \ll 1$ (e.g., for the traditional conductive fillers such as carbon fibers), the geometrical effect of the thin penetrable shell is negligible. Therefore, the percolation threshold can still be accurately predicted by the classic percolation theory, even though the saturation conductivity of the composites can be much lower than the electrical conductivity of the individual fillers [37]. However, for nanofillers (e.g., nanotubes and carbon black), their size could be close to or even smaller than δ in two or three dimensions and thus the effect of δ becomes significant. According to the literatures [13, 38, 39], the value of δ in the polymeric matrices may range from a few nanometers to several hundreds of nanometers. Such a wide distance range for the electron hopping was explained by the multistep hopping process [13]. Using values of 100 and 5 nm for δ, the foregoing theoretical value of the lowest percolation threshold will decrease from 0.34 to 0.02 vol.% and 0.2 vol.%, respectively. The results are in reasonable agreement with the experimental result (which is lower than 0.05 vol.%). The "hard-core" model can also explain the ultra low percolation threshold observed in carbon-black-filled polymers, e.g., 0.06 vol.% [40], whereas the theoretical value of percolation threshold for randomly dispersed, hard, spherical micro-particles has been

determined to be ~ 16 vol.% [9]. For example, when $\delta/D = 10$, the percolation threshold determined by the "hard-core" model will be 1000 times lower than that by the classic percolation theory. Nevertheless, although the "hard-core" model can qualitatively explain the conductive mechanism of the polymeric composites filled with conducting nanofillers, the quantitative calculation or simulation of the percolation threshold is still very hard due to the difficulty in defining the electron hopping distance and the morphology of aggregated nanofillers.

Conclusion

In this study, the electrical property of CNT/epoxy composites was investigated and analyzed with respect to the aspects of the percolation theory. The morphology of CNTs was characterized by using different microscopic techniques such as AFM, TEM, and SEM. On the basis of micro-observations, the effect of CNT distribution on the electrical behavior is discussed. In particular, the following conclusions can be drawn.

1. Multi-wall CNTs were dispersed into an epoxy matrix using a calendering approach, which led to an ultra low percolation threshold of below 0.05 vol.%. The electrical conductivity of the epoxy nanocomposites can be enhanced by more than nine orders of magnitude with the addition of 0.6 vol.% CNTs.
2. The electrical percolation behavior of CNT-filled epoxy composites shares the key features of percolation theory. This means, the conductivity abruptly changes with the formation of a percolation path at a critical concentration, and the following increase can be well described by a scaling law. Moreover, the tunneling effect between weakly connected CNTs appears to be the probable mechanism of electrical conduction in nanocomposites. The quality of tubes dispersion as well as the nature of the interaction between tubes and polymer matrix is crucial for the conductive properties of CNT-filled polymer systems.
3. The charge contrast SEM imaging is a very useful technique to visualize CNTs distribution in polymer composites, even on several length scales, from nanometers to micrometers. This will provide a solid base to achieve an in-depth understanding of the processing–structure–property relationships of CNT-filled nanocomposites.

Acknowledgements The authors are grateful to the IVW GmbH (CEO: Prof. Dr.-Ing. A. K. Schlarb) where most of the results were generated. The authors also acknowledge the help of the technicians, H. Gietzsch and S. Schmitt at the IVW, GmbH. L. Chang wishes to thank the Alexander von Humboldt-Foundation for the research fellowship at IVW during the year 2008, P. Toro appreciates the support of DAAD for his stay at IVW in 2006, and K. Friedrich is grateful to the Australian Research Council for his Professional Fellowship at the University of Sydney in 2006/2007.

References

1. Ijima S, Ichihashi T (1993) Nature 363:603
2. Baughman RH, Zakhidov AA, de Heer WA (2002) Science 297:787
3. Thostenson ET, Ren ZF, Chou TW (2001) Compos Sci Technol 61:1899
4. Andrews R, Weisenberger MC (2004) Curr Opin Solid State Mater Sci 8:31
5. Colbert DT (2003) Plast Addit Compound 5:18
6. Das N, Maiti S (2008) J Mater Sci 43:1920. doi:10.1007/s10853-008-2458-8
7. Stauffer D, Aharony A (1994) Introduction to percolation theory. Taylor and Francis, London
8. Weber M, Kamal MR (1997) Polym Compos 18:711
9. Kirkpatrick S (1973) Rev Mod Phys 45:574
10. Heo SI, Yun JC, OH KS, Han KS (2006) Adv Compos Mater 15:115
11. Balberg I, Anderson CH, Alexander S, Wagner N (1984) Phys Rev B 30:3933
12. Celzard A, McRae E, Deleuze C, Dufort M, Furdin G, Mareche JF (1996) Phys Rev B 53:6209
13. Dani A, Ogale AA (1996) Compos Sci Technol 56:911
14. Lu C, Mai YW (2008) J Mater Sci 43:6012. doi:10.1007/s10853-008-2917-2
15. Balberg I, Binenbaum N (1983) Phys Rev B 28:3799
16. Mclachlan DS, Chiteme C, Park C, Wise KE (2005) J Polym Sci B 43:3273
17. Kovacs JZ, Velagala BS, Schulte K, Bauhofer W (2007) Compos Sci Technol 67:922
18. Sandler J, Shaffer MP, Prasse T, Bauhofer W, Schulte K, Windle AH (1999) Polymer 40:5967
19. Sandler J, Kirk JE, Kinloch IA, Shaffer MP, Windle AH (2003) Polymer 44:5893
20. Barrau S, Demont P, Peigney A, Laurent C, Lacabanne C (2003) Macromolecules 36:5187
21. Martin CA, Sandler JKW, Shaffer MSP, Schwarz MK, Bauhofer W, Schulte K, Windle AH (2004) Compos Sci Technol 64:2309
22. Kim YJ, Shin TS, Choi HD, Kwon JH, Chung YC, Yoon HG (2005) Carbon 43:23
23. Thostenson ET, Chou TW (2006) Carbon 44:3022
24. Ionescu E, Francis A, Riedel R (2009) J Mater Sci 44:2055. doi:10.1007/s10853-009-3304-3
25. Bryning MB, Islam MF, Kikkawa JM, Yodh AG (2005) Adv Mater 17:1186
26. Kanetoa K, Tsurutaa M, Sakaia G, Chob WY, Andob Y (1999) Synth Met 103:2543
27. Gojny FH, Wichmann MHG, Fiedler B, Kinloch I, Bauhofer W, Windle AH, Schulte K (2006) Polymer 47:2036
28. Loos J, Alexeev A, Grossiord N, Koning C, Regev O (2005) Ultramicroscopy 104:160
29. Zhang HB, Feng RJ, Ura K (2004) Sci Prog 87:249
30. Dalmas F, Dendievel F, Chazeau L, Cavaille JY, Gauthier C (2006) Acta Mater 54:2923
31. Sheng P, Sichel EK, Gittleman JI (1978) Phys Rev Lett 40:1197
32. Balberg I (1987) Phys Rev Lett 59:1305
33. Ounaies Z, Park C, Wise KE, Siochi EJ, Harrison JS (2003) Compos Sci Technol 63:1637
34. Hu G, Zhao C, Zhang S, Yang M, Wang Z (2006) Polymer 47:480

35. Kilbride BE, Coleman JN, Fraysse J, Fournet P, Cadek M, Drury A, Hutzler S, Roth S, Blau WJ (2002) J Appl Phys 92:4024
36. Pötschke P, Abdel-Goad M, Alig I, Dudkin S, Lellinger D (2004) Polymer 45:8863
37. Tsotra P, Friedrich K (2003) Compos A Appl S 34:75
38. Du F, Scogna RC, Zhou W, Brand S, Fischer JE, Winey KI (2004) Macromolecules 37:9045
39. Aggarwal M, Khan S, Husain M, Ming TC, Tsai MY, Perng TP, Khan ZH (2007) Eur Phys J B 60:319
40. Schueler R, Petermann J, Schulte K, Wentzel HP (1997) J Appl Polym Sci 63:1741